Mutagenesis of Benzo[*a*]pyrene Diol Epoxide in Yeast: Requirement for DNA Polymerase ζ and Involvement of DNA Polymerase η[†]

Zhongwen Xie,[‡] Elena Braithwaite,[‡,§] Dongyu Guo,[‡] Bo Zhao,[‡] Nicholas E. Geacintov,[∥] and Zhigang Wang*,[‡]

Graduate Center for Toxicology, University of Kentucky, Lexington, Kentucky 40536, and Chemistry Department, New York University, New York, New York 10003

ABSTRACT: Benzo[*a*]pyrene is a potent environmental carcinogen, which can be metabolized in cells to the DNA damaging agent *anti*-benzo[*a*]pyrene-7,8-dihydrodiol-9,10-epoxide (*anti*-BPDE). We hypothesize that mutations induced by BPDE DNA adducts are mainly generated through an error-prone translesion synthesis that requires a specialized DNA polymerase (Pol). Using an in vivo mutagenesis assay in the yeast model system, we have examined the potential roles of Polζ and Polη in (±)-*anti*-BPDE-induced mutagenesis. In cells proficient in mutagenesis, (±)-*anti*-BPDE induced 85% base substitutions with predominant G → C followed by G → T transversions, 9% deletions of 1−3 nucleotides, and 6% insertions of 1−3 nucleotides. In *rad30* mutant cells lacking Polη, (±)-*anti*-BPDE-induced mutagenesis was reduced and accompanied by a moderate decrease in base substitutions and more significant decrease in deletions and insertions of 1−3 nucleotides. In *rev3* mutant cells lacking Polζ, (±)-*anti*-BPDE-induced mutagenesis was mostly abolished, leading to a great decrease in both base substitutions and deletions/insertions of 1−3 nucleotides. In contrast, large deletions/insertions were significantly increased in cells lacking Polζ. Consistent with the in vivo results, purified yeast Polζ performed limited translesion synthesis opposite (+)- and (−)-*trans-anti*-BPDE-N^2-dG DNA adducts with predominant G incorporation opposite the lesion. These results show that (±)-*anti*-BPDE-induced mutagenesis in yeast requires Polζ and partially involves Polη and suggest that Polζ directly participates in nucleotide insertions opposite the lesion, while Polη significantly contributes to deletions and insertions of 1−3 nucleotides.

DNA damage is a major cause of mutagenesis. In cells, error-prone lesion bypass constitutes a major mechanism of DNA damage-induced mutagenesis. Conceptually, lesion bypass can be divided into two steps: DNA synthesis opposite the template lesion and extension DNA synthesis beyond the lesion. During error-prone lesion bypass, the damaged site of DNA is directly copied, and an incorrect nucleotide is frequently incorporated opposite the lesion. In contrast, error-free lesion bypass predominantly incorporates the correct nucleotide opposite the lesion during translesion synthesis. Thus, error-free lesion bypass suppresses mutations, whereas error-prone lesion bypass promotes mutations following DNA damage.

Lesion bypass requires a specialized DNA polymerase (Pol)[1] to copy the damaged template (translesion synthesis). In eukaryotes, recent in vitro studies have demonstrated that Polζ (*1−3*), Pol*u* (*4, 5*), and the Y family DNA polymerases consisting of Polη, Polι, Polκ, and REV1 are capable of catalyzing translesion synthesis (reviewed in refs *6−10*).

However, it is mostly unknown whether these polymerases are actually recruited for translesion synthesis in vivo and to what extent each polymerase contributes to translesion synthesis with a given DNA lesion in cells. In vitro, translesion synthesis of a given lesion by the Y family DNA polymerases can be either error-free or error-prone depending on the specific polymerase, and translesion synthesis by a given Y family polymerase can be either error-free or error-prone depending on the specific lesion (reviewed in refs *7* and *8*). Thus, the genetic outcome resulting from the involvement of a Y family DNA polymerase in translesion synthesis in cells could be the suppression or promotion of damage-induced mutagenesis depending on the specific lesion. While in vitro biochemistry has yielded insightful information on mechanisms of DNA lesion bypass, understanding the contributions and roles of various specialized DNA polymerases in lesion bypass and mutagenesis in cells requires in vivo genetic analyses.

Benzo[*a*]pyrene, a potent carcinogen in animal models, is produced by the incomplete combustion of organic materials and is thus commonly found in the environment. In cells, benzo[*a*]pyrene is metabolically activated to highly reactive bay region dihydrodiol epoxide derivatives (*11, 12*). Racemic *anti*-benzo[*a*]pyrene-7,8-dihydrodiol-9,10-epoxide (*anti*-BPDE) are two such metabolites of benzo[*a*]pyrene, which react with DNA mainly at the N^2 position of guanine, forming stereoisomeric bulky adducts (+)-*trans-anti*-BPDE-N^2-dG, (+)-*cis-anti*-BPDE-N^2-dG, (−)-*trans-anti*-BPDE-N^2-

---

* Corresponding author. Tel.: (859) 323-5784. Fax: (859) 323-1059. E-mail: zwang@uky.edu.
‡ University of Kentucky.
§ Present address: NIEHS, Research Triangle Park, NC 27709.
∥ New York University.
[1] Abbreviations: Pol, DNA polymerase; BPDE, benzo[*a*]pyrene-7,8-dihydrodiol-9,10-epoxide; 5-FOA, 5-fluoroorotic acid; NER, nucleotide excision repair; nt, nucleotide.

dG, and (−)-*cis-anti*-BPDE-*N*²-dG (*12*, *13*). In cells, the major DNA adduct derived from benzo[*a*]pyrene is (+)-*trans-anti*-BPDE-*N*²-dG (*12*). In addition, minor BPDE DNA adducts are also formed, mainly at the *N*⁶ position of adenine (*12*). In vitro, the (+)- and (−)-*trans-anti*-BPDE-*N*²-dG lesions are effectively bypassed by human Polκ in an error-free manner (*14*−*16*). These findings predict that Polκ may function to suppress BPDE-induced mutagenesis in cells. This prediction has been confirmed recently by Ogi et al. (*17*). In contrast, human Polη performs error-prone translesion synthesis opposite (+)- and (−)-*trans-anti*-BPDE-*N*²-dG DNA adducts in vitro (*16*, *18*−*20*).

To understand mechanisms of BPDE-induced mutagenesis and to identify specific DNA polymerases involved in bypass of BPDE DNA adducts in cells, we have examined the potential roles of Polζ and Polη in the mutagenesis process in the yeast model system by using a combined biochemical and genetic approach. In this paper, we (i) describe an in vivo mutagenesis assay in yeast, (ii) demonstrate that Polζ is required for BPDE-induced mutagenesis, and (iii) show that Polη is involved in BPDE-induced mutagenesis as well, by especially contributing to induced frameshift mutagenesis involving 1−3 nucleotides.

EXPERIMENTAL PROCEDURES

Materials. Purified yeast Polη was obtained from Enzymax (Lexington, KY). Yeast Polζ (the Rev3−Rev7 complex) was purified to near homogeneity as previously described (*3*). A 33-mer DNA template containing either a (+)-*trans-anti*-*N*²-dG or a (−)-*trans-anti*-BPDE-*N*²-dG adduct was prepared as previously described (*21*−*23*). Its sequence is 5′-CTC-GATCGCTAAC<u>G</u>CTACCATCCGAATTCGCCC-3′, where the modified guanine is underlined. The (±)-*anti*-BPDE (98% purity) was purchased from the Midwest Research Institute (Kansas City, MO). Yeast strains used are BY4741-Δrad14 (proficient in mutagenesis) (*MATa his3 leu2 met15 ura3 rad14::HIS3*) and its isogenic BY4741Δrad14Δrad30 (*rad30* deletion mutant), BY4741Δrad14Δrev3 (*rev3* deletion mutant), and BY4741Δrad14Δrad30Δrev3 (*rad30 rev3* double deletion mutant).

BY4741 and BY4741Δrad30 (lacking Polη) strains were purchased from Research Genetics (Huntsville, AL). BY4741Δrev3 (lacking Polζ) was constructed by transforming BY4741 cells with a linearized *rev3* deletion plasmid construct that was provided by Christopher Lawrence (University of Rochester). The *rev3* deletion clone was confirmed by a functional assay demonstrating reduced UV-resistance and loss of UV-induced mutagenesis. The *rev3* deletion strain was further tested for complementation of UV resistance and UV-induced mutagenesis by a plasmid carrying the wild-type *REV3* gene. BY4741Δrad30Δrev3 (lacking both Polη and Polζ) was similarly constructed by transforming BY4741Δrad30 cells with the linearized *rev3* deletion plasmid construct and similarly confirmed for its *rev3* phenotype as described above. Finally, the *RAD14* gene of BY4741, BY4741Δrev3, and BY4741Δrad30Δrev3 was deleted by transforming the respective strains with a *rad14* deletion plasmid construct that was provided by Errol Friedberg (University of Texas Southwestern Medical Center at Dallas). The *rad14* deletion phenotype was confirmed by severe UV sensitivity of the respective cells followed by

complementation of UV resistance by the wild-type *RAD14* gene carried on a plasmid.

Preparation of BPDE-Damaged Plasmid DNA. Plasmid pCLU (50 μg) was incubated with 10 μM (±)-*anti*-BPDE in a 500-μL reaction mixture containing 20% ethanol and TE buffer (10 mM Tris-HCl, pH 7.5, 1 mM EDTA) for 3 h in the dark at 37 °C. The modified DNA was then purified by 5−20% sucrose gradient centrifugation at 28 000 rpm for 17 h at 4 °C in a Beckman SW41Ti rotor. Fractions of 0.5 mL each were collected from the bottom of the gradient and 5-μL aliquots were analyzed by electrophoresis on a 1% agarose gel to locate the DNA. Fractions containing supercoiled DNA were pooled, precipitated in ethanol, and dissolved in TE buffer. Treatment under these conditions generated on average about five lesions per kb DNA as determined by quantitative PCR (*24*). Thus, 36 DNA lesions on average were expected for each pCLU plasmid.

In Vivo Mutagenesis Assay in Yeast. Damaged or undamaged plasmid pCLU DNA (2 μg) was transformed into yeast cells of various strains by the lithium acetate method essentially as described (*25*). Immediately after transformation, yeast cells were collected by centrifugation (20 s at 5000 rpm) in a microcentrifuge and resuspended in 1 mL of sterile water. An aliquot (1 μL) of the cell suspension was diluted and plated onto YNB minimal agar plates (0.17% yeast nitrogen base, 0.49% ammonium sulfate, 2% glucose, and 2% agar) lacking leucine to score for plasmid survival (colonies containing replicated pCLU). The remaining cell suspension was directly plated onto three YNB minimal agar plates lacking leucine but supplemented with 5 mM 5-fluoroorotic acid (5-FOA), 150 μM methionine, and 380 μM uracil to score for colonies containing the *ura3* mutant pCLU. After incubation at 30 °C for 3−4 days, yeast colonies were counted. Mutation frequency was calculated by dividing the number of the *ura3* mutant colonies by the number of colonies containing replicated pCLU. Plasmid pCLU DNA was recovered from the *ura3* mutant colonies individually by a zymolyase method essentially as described (*26*) and used to transform *Escherichia coli* DH5α competent cells for plasmid amplification. Each mutant plasmid was then isolated from *E. coli*, followed by DNA sequencing to determine the precise *ura3* mutation.

DNA Polymerase Assays. A standard DNA polymerase reaction mixture (10 μL) contained 25 mM KH₂PO₄ (pH 7.0), 5 mM MgCl₂, 5 mM dithiothreitol, 100 μg/mL bovine serum albumin, 10% glycerol, 50 μM dNTPs (dATP, dCTP, dTTP, and dGTP individually or together as indicated), 50 fmol of a DNA template containing a ³²P-labeled primer, and purified Polζ or Polη as indicated. After incubation at 30 °C for 30 min, reactions were terminated with 7 μL of a stop solution (20 mM EDTA, 95% formamide, 0.05% bromophenol blue, and 0.05% xylene cyanol). The reaction products were resolved on a 20% polyacrylamide gel containing 8 M urea and visualized by autoradiography.

RESULTS

In Vivo Mutagenesis Assay in Yeast. To investigate mechanisms of BPDE-induced mutagenesis, we established an in vivo assay in the yeast *Saccharomyces cerevisiae* model system. This assay is derived from a method described by Roy and Fuchs (*27*). A similar mutagenesis assay was also
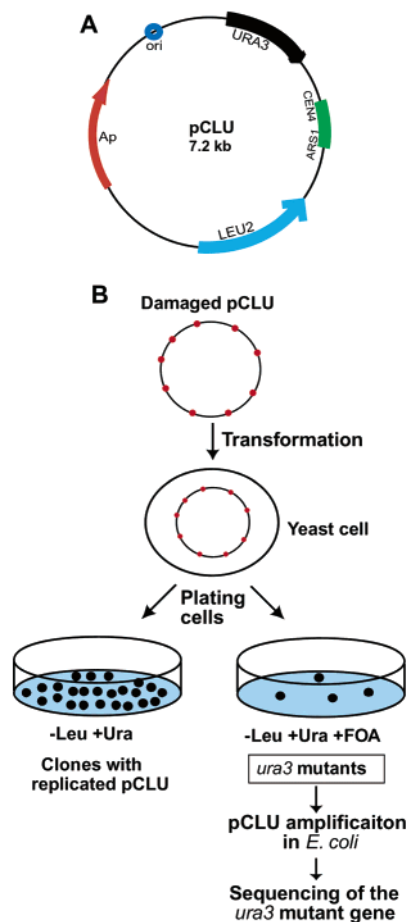
FIGURE 1: Schematic presentation of an in vivo mutagenesis assay in yeast. (A) Plasmid pCLU carrying the mutagenesis target gene *URA3*. The mutagenesis target size is 801 bp (open reading frame of *URA3*). *CEN4* and *ARS1*, sequence for autonomous replication in yeast; *LEU2*, selection marker in yeast cells; ori, replication origin in *E. coli*; Ap, ampicilin resistance gene. (B) Scheme of the plasmid-based mutagenesis assay in yeast cells. See text for details.
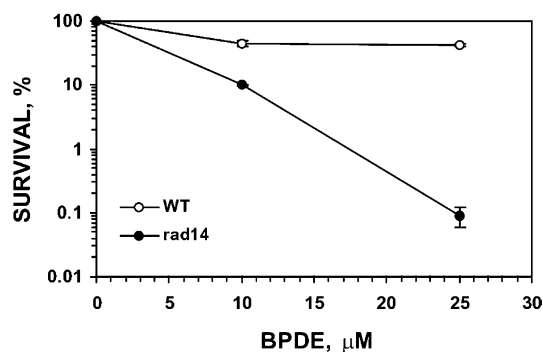

FIGURE 2: Effect of the NER repair function on survival of (±)-*anti*-BPDE-damaged plasmid in yeast cells. Equal amounts of undamaged and (±)-*anti*-BPDE-damaged plasmids were separately transformed into wild-type (WT) yeast cells or *rad14* deletion mutant cells lacking the NER repair function. Transformed cells were plated on minimal plates without leucine to score for colonies containing replicated plasmids. Plasmid survival, with the standard deviation shown, was calculated by dividing the number of damaged plasmid transformants by the number of undamaged plasmid transformants. Survival of the undamaged plasmid was taken as 100%.

developed in *E. coli* by Rodriguez and Loechler (*28*). In our mutagenesis assay, the plasmid pCLU was constructed, which contains the yeast *LEU2* gene as the plasmid selection marker and the yeast *URA3* gene as the 801-bp mutagenesis target (Figure 1A). Following in vitro treatment of pCLU with (±)-*anti*-BPDE, the damaged plasmid DNA was transformed into yeast cells. Transformed cells were plated on leucine-lacking minimal medium plates with or without 5-FOA. Plates without 5-FOA allowed cells that had replicated the damaged pCLU plasmid to grow to colonies, thus measuring the replication of the damaged plasmid (plasmid survival). Plates with 5-FOA allowed only those cells that contained inactivating mutations at the plasmid *URA3* gene to grow to colonies, thus measuring mutagenesis of the plasmid target gene. The mutation frequency was calculated by dividing the number of *ura3* mutant colonies by the number of colonies containing the replicated plasmid. The precise mutation was identified by sequencing the *ura3* mutant gene after recovering pCLU from the mutant colonies and amplifying the respective plasmids in *E. coli*. A schematic presentation of this in vivo mutagenesis assay is shown in Figure 1B.

Since BPDE DNA adducts are repaired by nucleotide excision repair (NER) (*24*, *29*), these lesions are subject to removal from pCLU when transformed into yeast cells.

Repair of BPDE DNA adducts by NER would allow efficient replication (survival) of the plasmid. Persistence of BPDE DNA adducts in pCLU would lead to reduced survival of the plasmid. To define a BPDE dose for in vitro damage of the pCLU plasmid, we first tested the survival of the damaged plasmid in wild-type BY4741 cells. As shown in Figure 2, the plasmid survival in wild-type cells was not significantly affected by BPDE treatment at a concentration as high as 25 μM. In contrast, following treatment by 25 μM BPDE, the plasmid survival was reduced by 1000-fold in *rad14* deletion mutant cells that lack NER function (Figure 2). These results suggest that BPDE adducts in the plasmid pCLU were effectively removed by NER in wild-type yeast cells. To detect BPDE-induced mutagenesis in the plasmid target in wild-type cells, we would have to employ much higher concentrations of (±)-*anti*-BPDE, which could potentially lead to a solubility problem and undesired DNA damage by contaminating compounds in the (±)-*anti*-BPDE preparation. Therefore, we chose to perform the mutagenesis assays in the absence of NER function (the *rad14* deletion genetic background), such that a relatively low concentration of 10 μM (±)-*anti*-BPDE could be used.

Effects of Polζ and Polη on (±)-Anti-BPDE-Induced Mutagenesis in Yeast. To determine whether Polζ and Polη affect BPDE-induced mutagenesis in vivo, we performed mutagenesis assays with yeast cells proficient in mutagenesis and cells lacking Polζ, Polη, or both. Untreated pCLU plasmid DNA was used in the assay as the control for spontaneous mutagenesis. In cells proficient in mutagenesis (*rad14*), replication efficiency of the pCLU plasmid damaged by 10 μM (±)-*anti*-BPDE was reduced to 10.2% as compared to that of the undamaged pCLU (Figure 3). In *rad30* mutant cells lacking Polη and *rev3* mutant cells lacking Polζ, replication of the (±)-*anti*-BPDE-damaged plasmid was further reduced to 4.6% (Figure 3). In cells lacking both Polη and Polζ (*rad14 rad30 rev3*), replication of the damaged plasmid was similarly reduced to 3.8% (Figure 3). These results suggest that both Polη and Polζ participate in the translesion replication of the (±)-*anti*-BPDE-damaged plasmid DNA in yeast cells.

Table 1: Spontaneous Mutations in Various Yeast Strains[a]

strain	base substitution $\times 10^{-4}$ (%)	deletion $\times 10^{-4}$ (%)		insertion[b] $\times 10^{-4}$ (%)		other[c] $\times 10^{-4}$ (%)	total $\times 10^{-4}$ (%)
		1−3 nt	>3 nt	1−3 nt	>3 nt		
rad14	3.5 (60)	1.0 (17)	0.8 (14)		0.4 (7)	0.1 (2)	5.8 (100)
rad14rad30	7.0 (54)		3.0 (23)		1.2 (9)	1.8 (14)	13 (100)
rad14rev3	8.7 (51)	1.4 (8)	4.6 (27)	0.7 (4)	1.7 (10)		17 (100)
rad14rad30rev3	3.9 (51)	0.6 (8)	2.7 (35)			0.4 (6)	7.6 (100)

[a] A total of 50, 20, 45, and 36 independent mutant clones from *rad14* (proficient in mutagenesis), *rad14 rad30* (lacking Polη), *rad14 rev3* (lacking Polζ), and *rad14 rad30 rev3* (lacking both Polη and Polζ), respectively, were sequenced. Mutation frequency is presented, followed by percentage of total mutations in the parentheses. [b] All insertions are duplicating insertions (i.e., exact sequence duplications), for example, GAAG → GAAAG; duplication of the nucleotide 29 to 143 of the *URA3* open reading frame, etc. [c] All other mutations are complex mutations containing a small duplicated *URA3* sequence, between which a large foreign sequence (about 100 bp or more) was inserted.
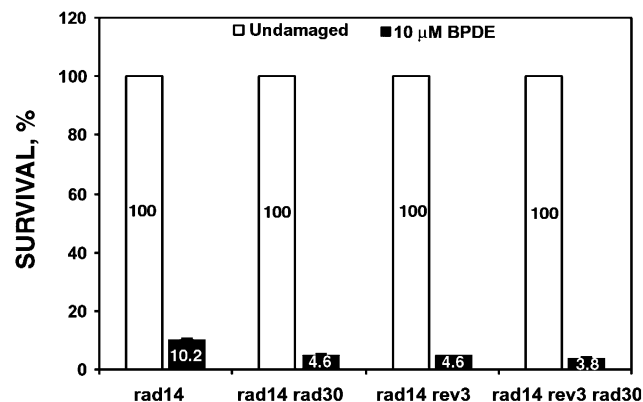

FIGURE 3: Effect of Polη and Polζ on replication of (±)-*anti*-BPDE-damaged plasmid in yeast cells. Equal amounts of undamaged and (±)-*anti*-BPDE-damaged plasmids were separately transformed into various yeast cells as indicated. Transformed cells were plated on minimal plates without leucine to score for colonies containing replicated plasmids. Plasmid survival, with the standard deviation shown, was calculated by dividing the number of damaged plasmid transformants by the number of undamaged plasmid transformants. Survival (replication efficiency) of the undamaged plasmid was taken as 100%. Each result is the average of at least three independent experiments. Open bar, undamaged plasmid; closed bar, damaged plasmid. *rad14*, proficient in mutagenesis; *rad14 rad30*, lacking Polη; *rad14 rev3*, lacking Polζ; *rad14 rad30 rev3*, lacking both Polη and Polζ.

We then determined the effect of Polη and Polζ on (±)-*anti*-BPDE-induced mutagenesis. As expected, in yeast cells proficient in mutagenesis, treatment of pCLU with 10 μM BPDE increased the mutation frequency of the plasmid *URA3* gene by ∼10-fold, as compared to the spontaneous mutation frequency (Figure 4). Without Polη, the BPDE-induced mutation frequency was reproducibly reduced by 1.4-fold ($P = 0.03$) to a level of ∼2.9-fold above the spontaneous mutation frequency (Figure 4). Without Polζ, the BPDE-induced mutation was largely abolished to a level of only ∼1.4-fold above the spontaneous mutation frequency (Figure 4). In the absence of both Polη and Polζ, the BPDE-induced mutation frequency was ∼1.8-fold above the spontaneous mutation frequency (Figure 4). These results show that Polζ is required for (±)-*anti*-BPDE-induced mutagenesis and that Polη contributes to a fraction of (±)-*anti*-BPDE-induced mutagenesis in yeast.

Alteration of the (±)-Anti-BPDE-Induced Mutation Spectrum by Polζ and Polη Activities. To identify the precise mutations of the *ura3* gene, we recovered mutant pCLU plasmids from each yeast colony, separately amplified them in *E. coli*, and then sequenced each plasmid clone. The types
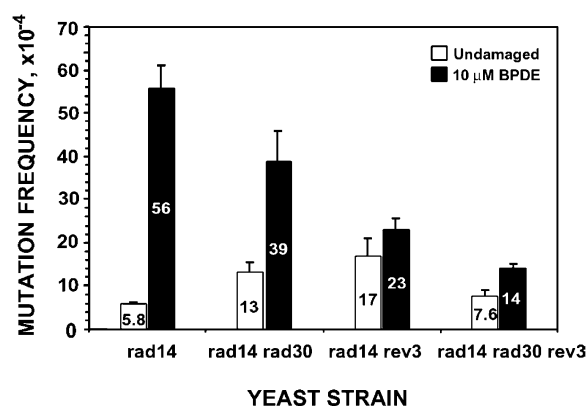

FIGURE 4: Mutagenesis induced by (±)-*anti*-BPDE in yeast cells of various strains. Using undamaged and (±)-*anti*-BPDE-damaged plasmid pCLU, in vivo mutagenesis assays were performed as described in the Experimental Procedures in yeast cells of various strains as indicated. Plasmid-transformed cells were plated on minimal plates without leucine and minimal plates supplemented with 5-FOA to score for colonies containing replicated plasmids and colonies containing plasmid *ura3* mutations, respectively. Mutation frequency was calculated by dividing the number of *ura3* mutant colonies by the number of colonies containing replicated plasmid (plasmid survival). Mutation frequencies with standard deviations of the undamaged (spontaneous mutagenesis, open bar) and damaged (closed bar) pCLU plasmid are shown. Each result is the average of three to six independent experiments. The difference of (±)-*anti*-BPDE-induced mutation frequency between *rad14* and *rad30* strains is statistically significant as determined by student's *t*-test ($p = 0.03$). *rad14*, proficient in mutagenesis; *rad14 rad30*, lacking Polη; *rad14 rev3*, lacking Polζ; *rad14 rad30 rev3*, lacking both Polη and Polζ.

of mutations observed were base substitutions, 1−3 nt deletions, >3 nt deletions, 1−3 nt insertions, >3 nt insertions, and complex mutations containing a small duplicated *URA3* sequence between which a large foreign sequence (about 100 bp or more) was inserted. Base substitutions and frameshift mutations of 1−3 nucleotides are shown in Figures 5 and 6 for spontaneous and (±)-*anti*-BPDE-induced mutagenesis, respectively. Base substitution mutations are detectable within a 787-bp region or 98% of the 801-bp *URA3* coding sequence (Figure 6).

In yeast cells proficient in mutagenesis (*rad14*), spontaneous base substitutions accounted for 60% of all mutations (Table 1). Three base substitution hot spots were apparent at positions 126 (G → C), 367 (G → C), and 446 (T → G), and one −1 deletion hot spot was found at position 446 (Figure 5). In cells lacking Polη or Polζ or both, the 126 and 367 hot spots and the 446−1 deletion hot spot disappeared (Figure 5). In cells lacking Polη, the 446 base

```
                                                               T
            10          20          30          40          50          60  C      70
     ATG TCG AAA GCT ACA TAT AAG GAA CGT GCT GCT ACT CAT CCT AGT CCT GTT GCT GCC AAG CTA TTT AAT ATC
                                                                                                  △
                                                                                                  △
                                                                                                △ △

                                                              C                  T
                                                            C C C              T T T
            80          90          100         110         120 C C   130      T         140
     ATG CAC GAA AAG CAA ACA AAC TTG TGT GCT TCA TTG GAT GTT CGT C ACC ACC AAG GAA TTA CTG GAG TTA GTT
                    △

                  G  C
            150   G  C   160         170         180         190         200   C    210
     GAA GCA TTA GGT CCC AAA ATT TGT TTA CTA AAA ACA CAT GTG GAT ATC TTG ACT GAT TTT TCC ATG GAG GGC

                          A           G                       A
            220         230         240         250         260         270 A   280
     ACA GTT AAG CCG CTA AAG GCA TTA TCC GCC AAG TAC AAT TTT TTA CTC TTC GAA GAC AGA AAA TTT GCT GAC

                                                C
     290         300         310         320         330         340         350     G   360
     ATT GGT AAT ACA GTC AAA TTG CAG TAC TCT GCG GGT GTA TAC AGA ATA GCA GAA TGG GCA GAC ATT ACG AAT
                                                         △

            C C C
            C C          C       C A              C C            T T           A
            C   370       C       C   380          C C   390      T   410           420         430
     GCA CAC GGT GTG GTG GGC CCA GGT ATT GTT AGC GGT TTG AAG CAG GCG GCA GAA GAA GTA ACA AAG GAA CCT
      △                 G G G G
                        G G G G
                        G
                        G G
        A  440   T   G G   450          460 A   T   470         480         490         500
     AGA GGC CTT TTG ATG TTA GCA GAA TTG TCA TGC AAG GGC TCC CTA TCT ACT GGA GAA TAT ACT AAG GGT ACT
        T       △                           △                                              △
                △ △
              △ △ △

     C
     C                                                                           T C
     A
     510         520     T   530         540         550         560     C    570
     GTT GAC ATT GCG AAG AGC GAC AAA GAT TTT GTT ATC GGC TTT ATT GCT CAA AGA GAC ATG GGT GGA AGA GAT

                   T                        C
                                            C C
     580         590         600            C  610       A  620         C  630         640
     GAA GGT TAC GAT TGG TTG ATT ATG ACA CCC GGT GTG GGT TTA GAT GAC AAG GGA GAC GCA TTG GGT CAA CAG
       ▲                                     △                                          △

                                                                  T
     650         660         670         680         690         700         710         720
     TAT AGA ACC GTG GAT GAT GTG GTC TCT ACA GGA TCT GAC ATT ATT ATT GTT GGA AGA GGA CTA TTT GCA AAG
                                                                  ▲

                                                   G                C              T
                    T                              G                C              T
            730     T   740         750            G  760         C A   770        T
     GGA AGG GAT GCT AAG GTA GAG GGT GAA CGT TAC AGA AAA GCA GGC TGG GAA GCA TAT TTG AGA AGA TGC GGC

     G
     G  800
     CAG CAA AAC
```
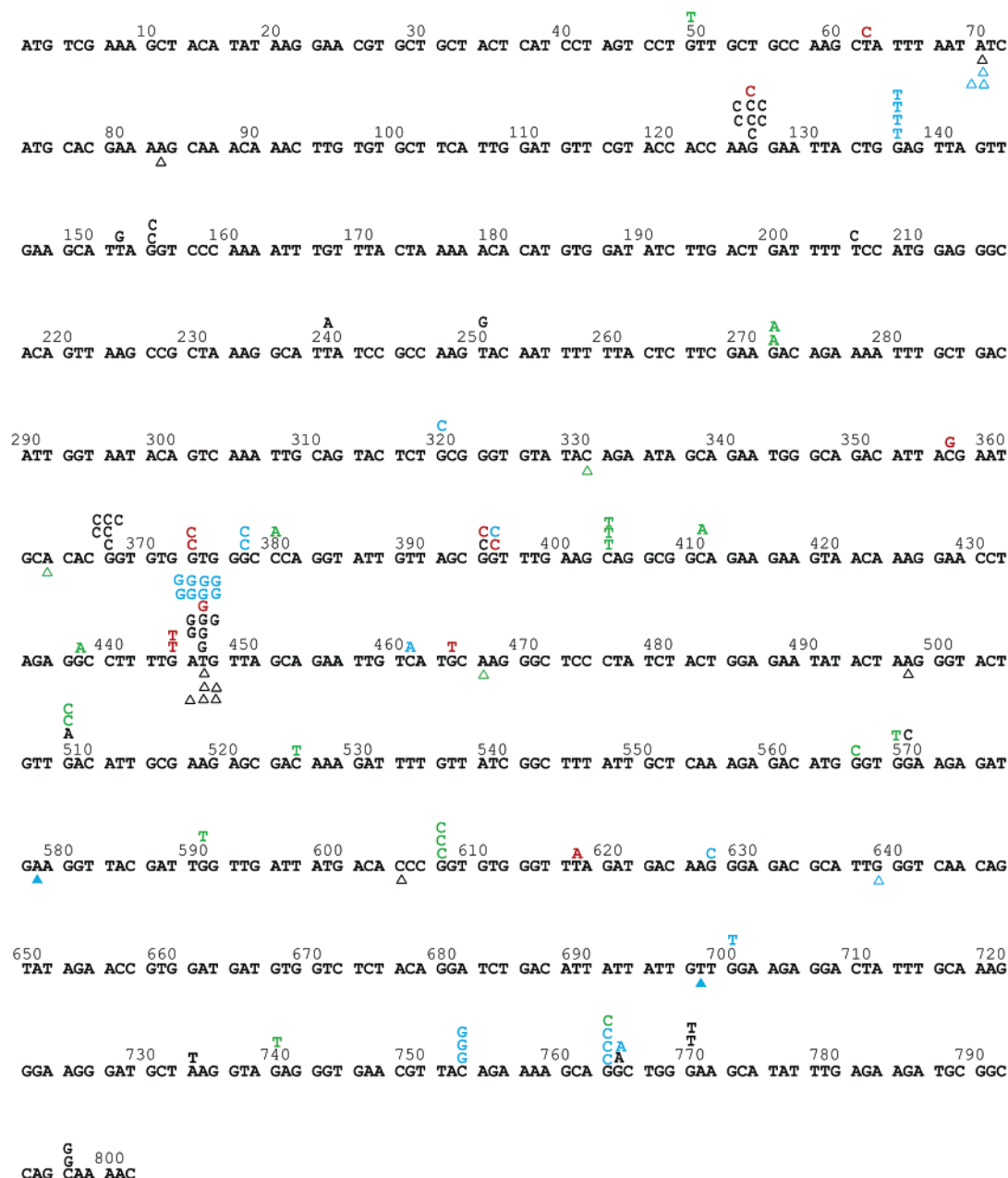
FIGURE 5: Spectrum of spontaneous mutagenesis at the plasmid *URA3* gene target. For simplicity, only base substitutions and frameshift mutations of 1−3 nucleotides are shown. While base substitutions are shown above the nucleotide sequence, deletions (open triangle) and insertions (filled triangle) are shown below the sequence. Black symbols, mutations in *rad14* cells (proficient in mutagenesis); red symbols, mutations in *rad14 rad30* cells (lacking Polη); blue symbols, mutations in *rad14 rev3* cells (lacking Polζ); green symbols, mutations in *rad14 rad30 rev3* cells (lacking both Polη and Polζ).

substitution hot spot additionally disappeared (Figure 5). Another major alteration of the spontaneous mutation spectrum as a result of deleting Polη, Polζ, or both was a significant increase in large fragment (>3 nt) frameshift mutations (Table 1). In some large deletion mutations, sequences of up to several hundred bp were deleted.

After treatment of the plasmid DNA with 10 μM (±)-*anti*-BPDE, the induced mutations consisted of 85% base substitutions, 9% deletions of 1−3 nucleotides, and 6% insertions of 1−3 nucleotides in yeast cells proficient in mutagenesis (Table 2). In *rad30* mutant cells (lacking Polη), while base substitutions were moderately reduced, both 1−3 nt deletions and insertions were more significantly reduced (Table 2). In cells proficient in mutagenesis or lacking Polη, most small frameshift mutations were 1 nucleotide deletions

and insertions. The −1 deletions occurred more frequently within single nucleotide repeats (Figure 6). All +1 insertions in these two strains occurred at A:T base pairs 5′ or 3′ to a G:C base pair (the presumed damage site) (e.g., 5′-ATTG → 5′-ATTTG and 5′-CAAA → 5′-CAAAA (Figure 6)). Base substitutions and small deletions and insertions were further reduced in cells lacking Polζ (Table 2). Furthermore, in *rev3* mutant cells (lacking Polζ), large insertions were dramatically increased (Table 2). Another major alteration of the (±)-*anti*-BPDE-induced mutation spectrum as a result of deleting Polη or Polζ was the shift of base substitution hot spots. Cells proficient in mutagenesis showed one weak hot spot at position 541 (Figure 6). Cells lacking Polη exhibited three hot spots at positions 605, 607, and 763 (Figure 6). Cells lacking Polζ showed one strong hot spot at position 268
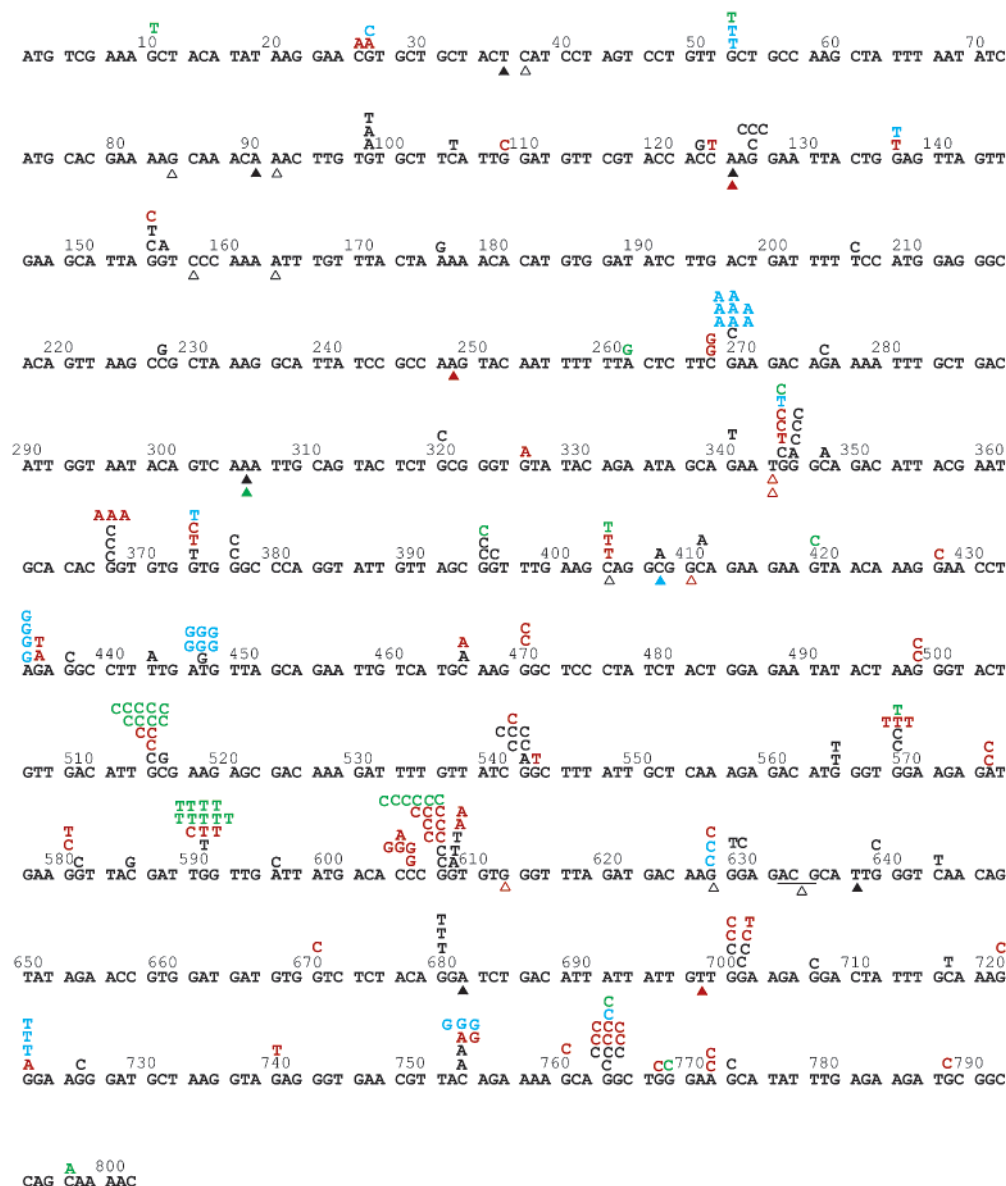
FIGURE 6: Spectrum of (±)-*anti*-BPDE-induced mutagenesis at the plasmid *URA3* gene target. For simplicity, only base substitutions and frameshift mutations of 1−3 nucleotides are shown. While base substitutions are shown above the nucleotide sequence, deletions (open triangle) and insertions (filled triangle) are shown below the sequence. The 3 nt deletion is indicated by an underline and an open triangle. Black symbols, mutations in *rad14* cells (proficient in mutagenesis); red symbols, mutations in *rad14 rad30* cells (lacking Polη); blue symbols, mutations in *rad14 rev3* cells (lacking Polζ); green symbols, mutations in *rad14 rad30 rev3* cells (lacking both Polη and Polζ).

Table 2: Mutations Induced by (±)-*anti*-BPDE in Various Yeast Strains[a]

		deletion $\times 10^{-4}$ (%)		insertion[b] $\times 10^{-4}$ (%)		other[c]	total
strain	base substitution $\times 10^{-4}$ (%)	1−3 nt	>3 nt	1−3 nt	>3 nt	$\times 10^{-4}$ (%)	$\times 10^{-4}$ (%)
rad14	48 (85)	5.0 (9)		3.4 (6)			56 (100)
rad14rad30	34 (88)	2.0 (5)	1.2 (3)	1.6 (4)			39 (100)
rad14rev3	14 (59)		6.7 (29)	0.5 (2)	1.6 (7)	0.7 (3)	23 (100)
rad14rad30rev3	9.4 (67)		3.5 (25)	0.3 (2)	0.6 (4)	0.3 (2)	14 (100)

[a] A total of 66, 60, 51, and 36 independent mutant clones from *rad14* (proficient in mutagenesis), *rad14 rad30* (lacking Polη), *rad14 rev3* (lacking Polζ), and *rad14 rad30 rev3* (lacking both Polη and Polζ), respectively, were sequenced. Mutation frequency is presented, followed by percentage of total mutations in the parentheses. [b] All insertions are duplicating insertions (i.e., exact sequence duplications), for example, TTG → TTT**G**; TAAAGGCATTATCCGC → TAAAGGCATTATCCGC**TAAAGGCATTATCCGC**, etc. [c] All other mutations are complex mutations containing a small duplicated *URA3* sequence, between which a large foreign sequence (about 100 bp or more) was inserted.

(G → A) and two other hot spots at positions 433 (A → G) and 446 (T → G) (Figure 6). Cells lacking both Polη and Polζ showed three strong hot spots at positions 514 (G → C), 590 (G → T), and 607 (G → C) (Figure 6). On the basis

of these results, we conclude that (i) (±)-*anti*-BPDE primarily induces base substitution mutations at the G−C base pairs; (ii) Polη significantly participates in 1−3 nucleotide deletions and insertions at sites of BPDE damage; and (iii)

Table 3: Base Substitution Specificity of Spontaneous Mutations in Various Yeast Strains[a]

	rad14 (%)	rad14 rad30 (%)	rad14 rev3 (%)	rad14 rad30 rev3 (%)
G → C	50.0	41.7	32.0	36.8
G → T	5.9	25.0	20.0	21.1
G → A	5.9		4.0	15.8
C → T				15.8
C → A				10.5
C → G	5.9	8.3	12.0	
A → C				
A → T	2.9			
A → G				
T → C	2.9	8.3	32.0	
T → A	2.9	8.3		
T → G	23.5	8.3		
total	100	100	100	100

[a] Independent *ura3* mutant clones derived from undamaged plasmid pCLU were sequenced (Table 1), and the precise base substitutions were compiled for each yeast strain as indicated. *rad14*, proficient in mutagenesis; *rad14 rad30*, lacking Polη; *rad14 rev3*, lacking Polζ; *rad14 rad30 rev3*, lacking both Polη and Polζ.

Table 4: Base Substitution Specificity of (±)-*anti*-BPDE-Induced Mutations in Various Yeast Strains[a]

	rad14 (%)	rad14 rad30 (%)	rad14 rev3 (%)	rad14 rad30 rev3 (%)
G → C	54.3	48.7	11.8	57.1
G → T	16.0	17.1	23.5	34.3
G → A	7.4	11.8	26.5	
C → T	3.7	3.9		2.9
C → A	7.4	3.9		2.9
C → G	4.9	9.2	8.8	
A → C	1.2	5.3		
A → T				
A → G	1.2		11.8	2.9
T → C	1.2			
T → A	1.2			
T → G	1.2		17.6	
total	100	100	100	100

[a] Independent *ura3* mutant clones derived from (±)-*anti*-BPDE-damaged plasmid pCLU were sequenced (Table 2), and the precise base substitutions were compiled for each yeast strain as indicated. *rad14*, proficient in mutagenesis; *rad14 rad30*, lacking Polη; *rad14 rev3*, lacking Polζ; *rad14 rad30 rev3*, lacking both Polη and Polζ.

the vast majority of base substitutions and 1−3 nt deletions and insertions require Polζ activity in yeast cells.

Base Substitution Specificity of (±)-Anti-BPDE-Induced Mutagenesis in Various Yeast Strains. Among the 12 possible base substitutions, G → C and T → G transversions were the first and second most frequent events in yeast cells proficient in mutagenesis (the *rad14* strain), accounting for 50 and 24%, respectively, of the total spontaneous point mutations (Table 3). In *rad30* mutant cells lacking Polη, the base substitution specificity was significantly altered in that both G → C and T → G mutations were reduced, while G → T mutations were increased to 25% (Table 3) of the total spontaneous point mutations. In *rev3* mutant cells lacking Polζ, G → C mutations were largely reduced (32%), whereas G → T and T → C mutations were significantly increased to 20 and 32%, respectively (Table 3). Similarly, in cells lacking both Polη and Polζ (*rev3 rad30*), G → C mutations were largely reduced (37%), whereas G → T mutations were significantly increased to 21% of the total spontaneous point mutations (Table 3). In addition, G → A, C → T, and C → A mutations were also increased (Table 3).

After treatment of the plasmid DNA with 10 μM (±)-*anti*-BPDE, G → C and G → T transversons constituted the most frequent base substitutions, accounting for 54 and 16%, respectively, of the total point mutations (Table 4). The BPDE-induced base substitution specificity in *rad30* mutant cells is similar to that in cells proficient in mutagenesis (Table 4). In *rev3* mutant cells, G → C mutations were dramatically reduced (12%), while G → A, A → G, and T → G mutations were significantly increased (Table 4). Furthermore, point mutations were more concentrated at a few sites rather than scattered throughout the *URA3* gene as was the case in cells proficient in mutagenesis (Figure 6). All T → G mutations occurred at one site in the sequence 5′-TTTGA**T**GTTAG-3′ (position 446); all A → G mutations occurred at one site in the sequence 5′-ACCTA**A**GAGGC-3′ (position 433); and 89% of all G → A mutations occurred at one site in the sequence 5′-CTTCG**A**AGA-3′ (position 268) (Figure 6), where the mutated base is underlined. In *rev3 rad30* cells lacking both

Polη and Polζ, mainly G → C and G → T mutations were observed (Table 4). These point mutations were even more concentrated at a few host spots (Figure 6). While 75% of all G → T mutations occurred at one site in the sequence 5′-GAT**T**G̲GTTGA-3′ (position 590), 75% of all G → C mutations occurred at two sites in the sequences 5′-ATT**G**C̲GAAG-3′ and 5′-CC**C**G̲GGTGT-3′ (positions 514 and 607, respectively) (Figure 6), where the mutated G is underlined. Remarkably, these base substitutions coincided with the same base (indicated in bold type in the sequences) 3′ or 5′ of the mutation site. We propose that these hot spot base substitutions in *rev3* mutant cells may be generated by duplicating the undamaged base 3′ to the lesion or looping out the lesion to copy the 5′ undamaged base followed by realigning the primer-template.

Specificity of In Vitro Translesion Synthesis by Yeast Polζ and Polη Opposite (±)-Trans-Anti-BPDE-N²-dG DNA Adducts. In yeast cells proficient in mutagenesis, the mutation frequency of (±)-*anti*-BPDE-damaged pCLU was 10-fold higher than that of the undamaged plasmid (Figure 4), and base substitutions predominated after BPDE damage (Table 2). Therefore, the majority (>90%) of base substitutions observed with the damaged plasmid in these cells resulted from translesion synthesis of the BPDE lesions. By comparing the in vivo base substitution specificity of (±)-*anti*-BPDE-induced mutagenesis (Table 4) with the in vitro base incorporation specificity of yeast Polζ opposite (±)-*trans*-*anti*-BPDE-N²-dG DNA adducts, we wished to gain insights into the role of Polζ in translesion synthesis in response to BPDE-guanine DNA adducts.

To perform in vitro translesion synthesis assays, we annealed a 5′ ³²P-labeled 19-mer primer terminating right before a template (+)- or (−)-*trans*-*anti*-BPDE-N²-dG adduct (Figure 7) and incubated this DNA substrate with purified yeast Polζ under standard DNA synthesis conditions. As shown in Figure 7A (lanes 1 and 6), purified yeast Polζ was able to perform limited translesion synthesis opposite (+)- and (−)-*trans*-*anti*-BPDE-N²-dG adducts. To determine which nucleotide was incorporated opposite the lesion by Polζ, DNA synthesis assays were performed in the presence
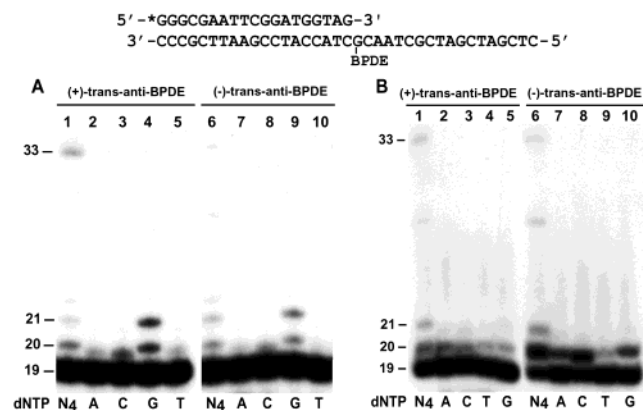
FIGURE 7: DNA synthesis by yeast Polζ and Polη from templates containing a site-specific (+)- or (−)-*trans-anti*-BPDE-N^2-dG adduct. A ^{32}P-labeled 19-mer primer was annealed to the damaged template with the primer 3′ end terminating right before the lesion as shown on the top. DNA synthesis assays were then performed in the presence of a single dATP (A), dCTP (C), dTTP (T), or dGTP (G), or all four dNTPs (N₄), using the damaged templates as indicated. Products of DNA synthesis were separated by 20% denaturing polyacrylamide gel and visualized by autoradiography of the gel. DNA size markers in nucleotides are indicated on the left. (A) DNA synthesis with 39 ng (193 fmol) of purified yeast Polζ. (B) DNA synthesis with 10 ng (141 fmol) of purified yeast Polη.

of only one deoxyribonucleoside triphosphate at a time. As shown in Figure 7A (lanes 4 and 9), a G was preferentially incorporated opposite the lesion, followed by another G incorporation opposite the undamaged template C immediately 5′ to the lesion. Less frequently, A and T were also incorporated opposite the (+)-*trans-anti*-BPDE-N^2-dG adduct (Figure 7A, lanes 2 and 5). Incorporation of the correct C opposite (+)- and (−)-*trans-anti*-BPDE-N^2-dG adducts was observed, but it occurred at a lower frequency than G misincorporation (Figure 7A, lanes 3 and 8). These results show that yeast Polζ is capable of limited error-prone translesion synthesis opposite (+)- and (−)-*trans-anti*-BPDE-N^2-dG DNA adducts in vitro. These in vitro results are consistent with the in vivo results that (±)-*anti*-BPDE-induced base substitutions require Polζ, resulting in predominant G → C mutations as a result of G misincorporation opposite the lesion.

In response to the (−)-*trans-anti*-BPDE-N^2-dG DNA adduct, purified yeast Polη most frequently inserted a C (Figure 7B, lane 8). Less frequently, a G and an A were also inserted opposite the lesion by Polη (Figure 7B, lanes 7, 9, and 10). However, translesion synthesis mostly stopped opposite the lesion (Figure 7B, lane 6). Translesion synthesis by yeast Polη was less efficient opposite the (+)-*trans-anti*-BPDE-N^2-dG adduct (Figure 7B, lane 1), the major BPDE DNA adduct in cells (*12*), than opposite the (−)-*trans-anti*-BPDE-N^2-dG adduct. Nevertheless, A and C were preferentially inserted by yeast Polη opposite the (+)-*trans-anti*-BPDE-N^2-dG (Figure 7B, lanes 3 and 4). Since Polη did not significantly affect the (±)-*anti*-BPDE-induced base substitution spectrum in vivo (Table 4) and was inefficient in inserting a nucleotide opposite the (+)-*trans-anti*-BPDE-N^2-dG adduct in vitro (Figure 7B, lanes 1−5), we conclude that Polη does not play a major role in catalyzing nucleotide insertions opposite (±)-*anti*-BPDE-induced DNA adducts in yeast cells.

DISCUSSION

In this study, we have examined the role of Polζ and Polη in translesion synthesis of (±)-*anti*-BPDE-induced DNA adducts in yeast cells. Translesion synthesis was examined by an in vivo mutagenesis assay, which directly measures error-prone translesion synthesis in cells. Thus, if the polymerase contributes to error-prone translesion synthesis in response to BPDE DNA adducts, the activity of this polymerase would stimulate BPDE-induced mutagenesis. If the polymerase contributes to error-free translesion synthesis, the activity of this polymerase would suppress BPDE-induced mutagenesis. Genetic analysis in yeast for in vivo roles of Polζ and Polη in translesion synthesis has a distinct advantage in that this organism does not contain any of the other two Y family DNA polymerases, Polι and Polκ. This greatly simplifies the interpretation of the genetic results.

In our plasmid-based mutagenesis assay, spontaneous mutagenesis was increased in the *rev3* mutant cells (Figure 4), in which an increase of large deletions and insertions made a major contribution (Table 1). Such deletions/insertions of large DNA fragments are likely generated by a recombination mechanism in yeast cells. The spontaneous recombination frequency is probably higher in the plasmid-based mutagenesis system when Polζ is inactivated, although the precise mechanism by which recombination may be stimulated in the absence of the Polζ mutagenesis pathway is not known at the present time.

Mutagenesis induced by (±)-*anti*-BPDE in yeast cells lacking the NER repair function was readily detected in the plasmid *URA3* gene. Furthermore, inactivating point mutations were detected from nucleotide 10−796, covering a 787-bp region or 98% of the 801-bp open reading frame. Thus, the *URA3* gene provides a big target containing a large variety of sequence contexts for mutagenesis analyses. Nevertheless, since the mutagenesis assay is based on inactivation of the *URA3* gene, mutations that do not affect the activity of the Ura3 protein are not detectable. Base substitutions at the third position of codons are presumably more difficult to detect because some point mutations at such positions do not lead to a change of the amino acid sequence. Thus, like other forward mutagenesis systems, our *URA3* gene-based mutagenesis assay could be potentially biased toward certain types of base substitutions in response to some DNA damaging agents. Accordingly, we emphasize the importance of performing relative comparisons for a change in base substitution specificity among the various yeast strains (Table 4).

Consistent with the fact that (±)-*anti*-BPDE mainly forms covalent adducts at guanine residues in DNA (*12*), we observed base substitutions at the G−C base pairs as the major mutational events. A small fraction of mutations occurred at the A−T base pairs. This probably resulted from translesion synthesis of the BPDE-dA adducts, which are known as minor BPDE lesions in DNA (*12*). Base substitutions at G residues occurred mostly on the coding strand of the *URA3* gene. Since yeast cells used in these experiments are completely deficient in NER, such a strand bias in mutagenesis cannot be attributed to preferential repair of the transcribed strand. It is possible that cells may respond to BPDE-dG adducts somewhat differently depending on whether the lesion is located on the leading or the lagging

strand during replication. Strand bias has also been observed before in the case of UV-induced mutagenesis (*30*).

In yeast cells proficient in mutagenesis, (±)-*anti*-BPDE-induced mutations consisted of 85% base substitutions and 15% frameshift mutations. If Polζ plays a major role in nucleotide insertion opposite BPDE-dG DNA adducts, then the specificity of (±)-*anti*-BPDE-induced base substitutions in cells should reflect the intrinsic base insertion specificity of purified Polζ. Indeed, the preferential incorporation of G opposite (+)- and (−)-*trans-anti*-BPDE-N^2-dG adducts by Polζ in vitro is consistent with the predominant G → C mutations induced by (±)-*anti*-BPDE in vivo. It is likely that Polζ directly participates in nucleotide insertion opposite BPDE-dG adducts. Frameshift mutations that generate deletions or insertions of 1−3 nucleotides also largely depended on Polζ activity (Table 2). Most recently, Li et al. (*31*) reported that (±)-*anti*-BPDE-induced mutagenesis is largely abolished in cultured human cells expressing *hREV3* antisense RNA. Thus, a major role of Polζ in (±)-*anti*-BPDE-induced mutagenesis is apparently conserved from yeast to humans. In the absence of Polζ, deletions and insertions of large DNA fragments were significantly increased (Table 2), which probably resulted from recombination. It is possible that yeast cells may increasingly rely on recombination to relieve replication blockage by DNA lesions in the absence of the major Polζ translesion synthesis mechanism.

Previously, we reported that translesion synthesis by purified yeast Polζ was very weak in response to the (+)-*trans-anti*-BPDE-N^2-dG adduct (*16*). More efficient translesion synthesis of this lesion was observed with purified Polζ in this study (Figure 7A). This difference is attributable to somewhat higher enzymatic activity of Polζ used in this study, as freshly prepared enzyme was used. Nevertheless, the overall activity of translesion synthesis using purified Polζ was still limited (Figure 7A). Similarly, Polζ also performed limited translesion synthesis opposite a template AAF-adducted guanine and TT (*6−4*) photoproduct (*3*). It is likely that accessory factors may be required for efficient translesion synthesis by Polζ in cells. In *E. coli*, translesion synthesis by DNA polymerase V is indeed stimulated by its accessory factors (*32, 33*). It is of great interest to identify such putative accessory factors of Polζ in future studies.

We found that Polη contributes to (±)-*anti*-BPDE-induced mutagenesis in yeast, as indicated by a reduction of the induced mutation frequency in *rad30* mutant cells. Analysis of the types of mutations in *rad30* mutant cells revealed a significant decrease of 1−3 nucleotide deletions and insertions. Thus, Polη plays a significant role in generating small frameshift mutations in response to BPDE DNA adducts. Since *rev3* mutant cells are as deficient as *rev3 rad30* double mutant cells in generating 1−3 nucleotide frameshift mutations in (±)-*anti*-BPDE mutagenesis, the function of Polη in the frameshift synthesis process most likely requires Polζ activity. Surprisingly, purified yeast Polη is inefficient in responding to the (+)-*trans-anti*-BPDE-N^2-dG adduct. This is in contrast to human Polη, which readily performs translesion synthesis opposite this lesion positioned in the identical sequence context (*16, 18, 19*). The in vitro results with purified yeast Polη are consistent with in vivo mutagenesis results in that (±)-*anti*-BPDE-induced base substitution spectrum in *rad30* mutant cells is similar to that in cells proficient in mutagenesis. Hence, Polη is unlikely to
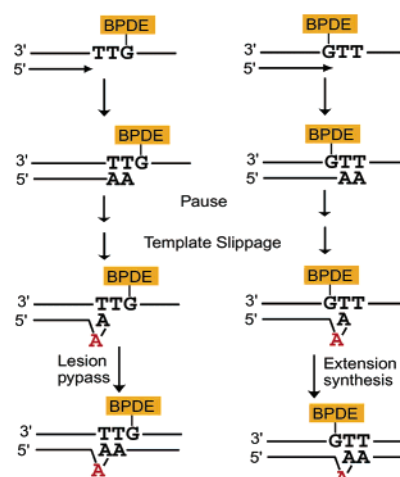

FIGURE 8: Mechanistic model of +1 insertion mutations induced by (±)-*anti*-BPDE in yeast cells. The sequence contexts were taken from two +1 insertion mutations observed. Scheme on the left, +1 insertion at the A:T base pair 3′ to the presumed G:C lesion site; scheme on the right, +1 insertion at the A:T base pair 5′ to the presumed G:C lesion site.

play a major role in catalyzing nucleotide insertions opposite BPDE-dG adducts in yeast cells. However, it is possible that Polη may play a noncatalytic role by promoting translesion synthesis of BPDE DNA adducts by other polymerases.

We noticed that +1 insertions induced by (±)-*anti*-BPDE in cells containing Polζ occurred at unique sequence contexts: duplicating an A:T base pair 5′ or 3′ to a G:C base pair, the presumed BPDE-dG adduct site. We propose the following mechanism to account for these unique +1 duplicating insertions. As a result of kinetically slowed reactions of nucleotide insertion opposite the BPDE-dG adduct or extension synthesis from opposite the lesion, the template is more likely to slip at the primer 3′ end. Such template slippage would be more profound when the primer ends at an A:T base pair due to its lower hydrogen bonding energy (two hydrogen bonds) as compared to a G:C base pair (three hydrogen bonds). Template slippage would then lead to +1 duplicating insertions as schematically presented in Figure 8. This model predicts that tandem mutations could be generated that contain a base substitution at the damaged G:C base pair and +1 duplicating insertion on its 5′ or 3′ side. Indeed, this type of tandem mutation was observed in yeast cells proficient in mutagenesis or lacking Polη (e.g., 5′-ACCAA → 5′-ACGAAA).

Our studies identified Polζ as the major polymerase and Polη as a minor polymerase in error-prone translesion synthesis of (±)-*anti*-BPDE DNA adducts in yeast cells. The (±)-*anti*-BPDE-induced frameshift of 1−3 nucleotides, however, significantly involves the Polη activity. It is also possible that Polη may additionally facilitate (±)-*anti*-BPDE-induced mutagenesis without directly catalyzing nucleotide insertions opposite the BPDE DNA adducts. Hence, at least two DNA polymerases participate in the bypass of BPDE DNA adducts in yeast cells, although each polymerase does not equally contribute to the process. Translesion synthesis of TT (6-4) photoproducts and AAF-adducted guanines also involve both Polζ and Polη in yeast cells (*34, 35*). Such a multiple-polymerase mode of translesion synthesis in cells may represent a general rather than an exceptional mechanism, as it provides better efficiency and some levels of

functional redundancy when copying the damaged DNA template.

REFERENCES

1. Nelson, J. R., Lawrence, C. W., and Hinkle, D. C. (1996) *Science 272*, 1646−1649.
2. Nelson, J. R., Lawrence, C. W., and Hinkle, D. C. (1996) *Nature 382*, 729−731.
3. Guo, D., Wu, X., Rajpal, D. K., Taylor, J.-S., and Wang, Z. (2001) *Nucleic Acids Res. 29*, 2875−2883.
4. Zhang, Y., Wu, X., Guo, D., Rechkoblit, O., Taylor, J. S., Geacintov, N. E., and Wang, Z. (2002) *J. Biol. Chem. 277*, 44582−44587.
5. Havener, J. M., McElhinny, S. A., Bassett, E., Gauger, M., Ramsden, D. A., and Chaney, S. G. (2003) *Biochemistry 42*, 1777−1788.
6. Ohmori, H., Friedberg, E. C., Fuchs, R. P. P., Goodman, M. F., Hanaoka, F., Hinkle, D., Kunkel, T. A., Lawrence, C. W., Livneh, Z., Nohmi, T., Prakash, L., Prakash, S., Todo, T., Walker, G. C., Wang, Z., and Woodgate, R. (2001) *Mol. Cell 8*, 7−8.
7. Wang, Z. (2001) *Mutat. Res. 486*, 59−70.
8. Wang, Z. (2001) *Mol. Interv. 1*, 269−281.
9. Livneh, Z. (2001) *J. Biol. Chem. 276*, 25639−25642.
10. Friedberg, E. C., Fischhaber, P. L., and Kisker, C. (2001) *Cell 107*, 9−12.
11. Phillips, D. H., and Grover, P. L. (1994) *Drug Metab. Rev. 26*, 443−467.
12. Peltonen, K., and Dipple, A. (1995) *J. Occup. Environ. Med. 37*, 52−58.
13. Cheng, S. C., Hilton, B. D., Roman, J. M., and Dipple, A. (1989) *Chem. Res. Toxicol. 2*, 334−340.
14. Zhang, Y., Yuan, F., Wu, X., Wang, M., Rechkoblit, O., Taylor, J.-S., Geacintov, N. E., and Wang, Z. (2000) *Nucleic Acids Res. 28*, 4138−4146.
15. Zhang, Y., Wu, X., Guo, D., Rechkoblit, O., and Wang, Z. (2002) *DNA Repair 1*, 559−569.
16. Rechkoblit, O., Zhang, Y., Guo, D., Wang, Z., Amin, S., Krzeminsky, J., Louneva, N., and Geacintov, N. E. (2002) *J. Biol. Chem. 277*, 30488−30494.
17. Ogi, T., Shinkai, Y., Tanaka, K., and Ohmori, H. (2002) *Proc. Natl. Acad. Sci. U.S.A. 99*, 15548−15553.
18. Zhang, Y., Yuan, F., Wu, X., Rechkoblit, O., Taylor, J.-S., Geacintov, N. E., and Wang, Z. (2000) *Nucleic Acids Res. 28*, 4717−4724.
19. Zhang, Y., Wu, X., Guo, D., Rechkoblit, O., Geacintov, N. E., and Wang, Z. (2002) *Mutat. Res. 510*, 23−35.
20. Chiapperino, D., Kroth, H., Kramarczuk, I. H., Sayer, J. M., Masutani, C., Hanaoka, F., Jerina, D. M., and Cheh, A. M. (2002) *J. Biol. Chem. 277*, 11765−11771.
21. Cosman, M., Ibanez, V., Geacintov, N. E., and Harvey, R. G. (1990) *Carcinogenesis 11*, 1667−1672.
22. Geacintov, N. E., Cosman, M., Mao, B., Alfano, A., Ibanez, V., and Harvey, R. G. (1991) *Carcinogenesis 12*, 2099−2108.
23. Rechkoblit, O., Amin, S., and Geacintov, N. E. (1999) *Biochemistry 38*, 11834−11843.
24. Braithwaite, E., Wu, X., and Wang, Z. (1998) *Carcinogenesis 19*, 1239−1246.
25. Becker, D. M., and Guarente, L. (1991) *Methods Enzymol. 194*, 182−187.
26. Strathern, J. N., and Higgins, D. R. (1991) *Methods Enzymol. 194*, 319−329.
27. Roy, A., and Fuchs, R. P. (1994) *Mol. Gen. Genet. 245*, 69−77.
28. Rodriguez, H., and Loechler, E. L. (1993) *Carcinogenesis 14*, 373−383.
29. Hess, M. T., Gunz, D., Luneva, N., Geacintov, N. E., and Naegeli, H. (1997) *Mol. Cell. Biol. 17*, 7069−7076.
30. McGregor, W. G., Wei, D., Maher, V. M., and McCormick, J. J. (1999) *Mol. Cell. Biol. 19*, 147−154.
31. Li, Z., Zhang, H., McManus, T. P., McCormick, J. J., Lawrence, C. W., and Maher, V. M. (2002) *Mutat. Res. 510*, 71−80.
32. Tang, M., Pham, P., Shen, X., Taylor, J. S., O'Donnell, M., Woodgate, R., and Goodman, M. F. (2000) *Nature 404*, 1014−1018.
33. Reuven, N. B., Arad, G., Stasiak, A. Z., Stasiak, A., and Livneh, Z. (2001) *J. Biol. Chem. 276*, 5511−5517.
34. Zhang, H., and Siede, W. (2002) *Nucleic Acids Res. 30*, 1262−1267.
35. Bresson, A., and Fuchs, R. P. (2002) *EMBO J. 21*, 3881−3887.